Controlling multidimensional off-resonant-Raman and infrared vibrational spectroscopy by finite pulse band shapes

Shaul Mukamel[a)]
Department of Chemistry, University of California, Irvine, California 92697-2025, USA

(Received 10 November 2008; accepted 18 December 2008; published online 4 February 2009)

Closed expressions are derived which incorporate pulse shaping effects in femtosecond nonlinear optical signals involving various combinations of temporally well-separated vibrationally resonant infrared and electronically off-resonant Raman pulses. Combinations of broadband and narrow band pulses that yield multidimensional extensions of coherent anti-Stokes Raman and sum frequency generation spectroscopy are presented. © *2009 American Institute of Physics*.
[DOI: 10.1063/1.3068548]

I. INTRODUCTION

Raman resonances are created when a difference of two optical frequencies coincides with a molecular vibrational transition. Such resonances carry useful information about vibrational frequencies and may be used to monitor energy-transfer pathways.[1–6] Purely vibrational dynamics is best studied by keeping all optical frequencies away from electronic resonances. Impulsive electronically off-resonance-Raman (EOR) signals $S^{(n)}$ generated by n very short ($\sim$50 fs) pulses depend parametrically on the time delays between pulses and are given by multipoint correlation functions of the electronic polarizability α,

$$S^{(3)}(t_1) \sim \frac{i}{h}\,[\alpha(t_1),\alpha(0)]\rangle, \tag{1}$$

$$S^{(5)}(t_2,t_1) \sim \frac{i}{h}\langle[[\alpha(t_2+t_1),\alpha(t_1)],\alpha(0)]\rangle, \tag{2}$$

$$S^{(7)}(t_3,t_2,t_1) \sim \frac{i}{h}\langle[[[\alpha(t_1+t_2+t_3),\alpha(t_1+t_2)],\alpha(t_1)],\alpha(0)]\rangle. \tag{3}$$

$S^{(3)}$ represents coherent anti-Stokes Raman spectroscopy (CARS) four wave mixing, which depends on a single time delay and is thus a one-dimensional (1D) technique.[1–4] Four-wave mixing is generally a three-dimensional (3D) technique by virtue of the three independent time delay variables between four pulses. However, under EOR conditions, two of these variables involve off-resonant electronic coherence and are thus very short. This leaves only one relevant time variable, whose frequency conjugate Ω [see Eq. (13)] reveals the Raman resonances. $S^{(5)}$ [see Eq. (19)] is the six wave mixing two-dimensional (2D) technique proposed by Tanimura and Mukamel[7] and realized experimentally in molecular liquids,[8–11] whereas $S^{(7)}$ is the 3D eight wave mixing Raman analog of the photon echo technique proposed by Loring and Mukamel[12] and also measured in molecular liquids.[13,14] These impulsive signals are independent of pulse shapes and profiles. The only control parameters are the time delays between pulses. EOR spectroscopy has been first carried out in the frequency domain using long (nanosecond) pulses.[3] Picosecond EOR spectra were used in the seventies to probe vibrational dephasing in the time domain.[1,2] Combinations of impulsive broadband and long narrow band pulses have been recently employed to manipulate these signals.[15–19] Resonant infrared (IR) signals are given by analogous expressions to Eqs. (1)–(3) obtained by simply replacing α with the dipole operator V. Equations (1)–(3) then represent $S^{(1)}$ (1D), $S^{(2)}$ (2D), and $S^{(3)}$ (3D), respectively.

Two ultrafast nonlinear spectroscopic techniques are widely used to study molecular vibrations. The first is sum frequency generation (SFG) performed with one resonant IR pulse followed by an EOR visible pulse.[20–24] The second, CARS, only uses visible EOR pulses.[15–19,25]

Generally the calculation of nonlinear signals with finite pulse envelopes requires multiple time integrations, which complicates the simulation and analysis. However, Schweigert and Mukamel[26] derived closed expressions for measurements involving resonant temporally well-separated pulses that revealed their dependence on both pulse delays and envelopes. Pulse shaping techniques may be used to design new signals by providing additional degrees of control over excitation conditions. These may simply involve pulse chirping or more elaborate pulse envelopes. In this article we show how measurements involving pairs of off-resonant Raman excitations can be analyzed in a similar fashion by introducing two-photon envelopes. Various possible pulse sequences involving EOR and vibrationally resonant IR pulses[27,28] are described and their information contents are compared and calculated. We demonstrate that heterodyne detection,[29–31] finite bandwidths, and frequency dispersion of the signal field can increase the dimensionality of the signals.[32] Narrow band detection, for example, may turn Eq. (1) from 1D into a 2D technique.

[a)]Electronic mail: smukamel@uci.edu.

II. MULTIDIMENSIONAL EXTENSIONS OF SUM FREQUENCY GENERATION AND OFF-RESONANCE CARS

The signal field $\varepsilon_s(\omega)$ [or $\varepsilon_s(t)$] is the ultimate observable in nonlinear spectroscopy. In heterodyne detection the field is interferometrically mixed with another strong (local oscillator) field $\varepsilon^*_{\mathrm{LO}}$ yielding[3,26–28] the frequency-dispersed signal.

$$S_{\mathrm{FD}}(\omega) = \mathrm{Re}[\varepsilon^*_{\mathrm{LO}}(\omega)\varepsilon_s(\omega)]. \tag{4}$$

In the time domain we similarly have the integrated signal

$$S_I = \int dt\ \mathrm{Re}[\varepsilon^*_{\mathrm{LO}}(t)\varepsilon_s(t)]. \tag{5}$$

The two detection modes are related by an integration

$$S_I = \int d\omega S_{\mathrm{FD}}(\omega). \tag{6}$$

The signal field can be recast in terms of the nth order nonlinear response function which, in turn, depends on the following type of integrals:[3,32]

$$\int_{-\infty}^{\tau_{n+1}} d\tau_n \int_{-\infty}^{\tau_n} d\tau_n \cdots \int_{-\infty}^{\tau_2} d\tau_1 \langle V(\tau_{v_{n+1}}) \cdots V(\tau_{v_1})\rangle \times \varepsilon_1(\tau_1)\cdots\varepsilon_n(\tau_n), \tag{7}$$

where V is the dipole operator, $\varepsilon_j(\tau)$ is the jth pulse envelope, and $\tau_1 \le \tau_2 \cdots \le \tau_{n+1}$ are time-ordered variables. τ_{n+1} is the observation time and $v_1 \cdots v_{n+1}$ is some permutation of the indices $1 \cdots n+1$. Because of this permutation, the time arguments within the multipoint dipole correlation functions in Eq. (7) are not ordered chronologically. We shall present expressions for various heterodyne-detected signals which show explicitly the dependence on both the pulse delays and bandwidths. The derivations involve various modular building blocks used for breaking up the multiple integrations in Eq. (7). For clarity these are given in the Appendix.

A. Infrared/infrared SFG

This is a $\chi^{(2)}$ process involving two incoming fields, $\mathbf{k}_1$ and $\mathbf{k}_2$, which generate a signal at $\mathbf{k}_3 = \mathbf{k}_1 + \mathbf{k}_2$. We denote the pulse envelopes as $\varepsilon_1(\omega), \varepsilon_2(\omega)$ and the local oscillator $\varepsilon(\omega)$. We consider the level scheme shown in Fig. 1(a) and assume that all three fields are resonant. We can then use Eq. (A2) to get for the heterodyne-detected signal

$$S_{\mathrm{IR,SFG}}(\Omega_2,\Omega_1) = \mathrm{Im}\sum_{a,b,c} P(a)\frac{V_{ac}V_{cb}V_{ba}}{(\Omega_2-\omega_{ca})(\Omega_1-\omega_{ba})} \times \varepsilon_3(\omega_{ac})\varepsilon_2(\omega_{cb})\varepsilon_1(\omega_{ba}), \tag{8}$$

where ω_{nm} is the frequency of the nm transition and V_{nm} is the corresponding dipole moment. $P(a)$ is the equilibrium population of state a, and Ω_1 and Ω_2 are Fourier conjugates to the two time delays, t_1 and t_2, shown in Fig. 1. Equation (8) reveals the information carried out by varying the pulse delays thorough Ω_1 and Ω_2 in the denominators and by the three pulse envelopes. Each transition is multiplied by a pulse envelope $\varepsilon_j(\omega)$ whose bandwidth controls the allowed transitions. Impulsive (broadband) pulses have flat frequency-independent envelopes.

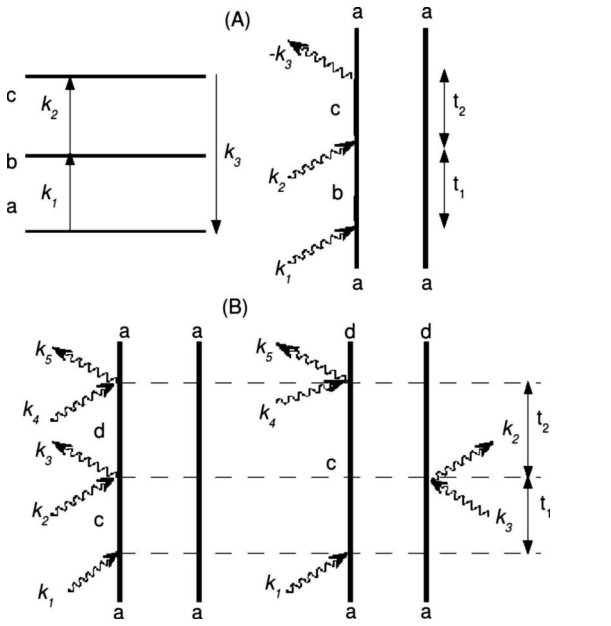

FIG. 1. (a) Level-scheme and Feyman diagram for all-IR sum-frequency-generation $\chi^{(2)}$ process [Eq. (8)]. (b) Feyman diagram for the IR/Raman/Raman $\chi^{(4)}$ process [Eq. (12)].

B. Infrared/Raman SFG

This $\chi^{(2)}$ process involves one resonant IR pulse followed by a single EOR pulse.[20–24,33–36] The signal generated at $\mathbf{k}_3 = \mathbf{k}_1 + \mathbf{k}_2$ is represented by the diagram in Fig. 2(a). The integrated heterodyne signal is obtained by using Eq. (A2) for ε_1 and Eq. (A9) for fields ε_2 and ε_3,

$$S_{\mathrm{SFG}}(\Omega_1) = \mathrm{Im}\sum_{a,c} P(a)\frac{\alpha_{ca}V_{ca}f_{32}(\omega_{ca})\varepsilon_1(\omega_{ca})}{\Omega_1-\omega_{ca}}. \tag{9}$$

Here

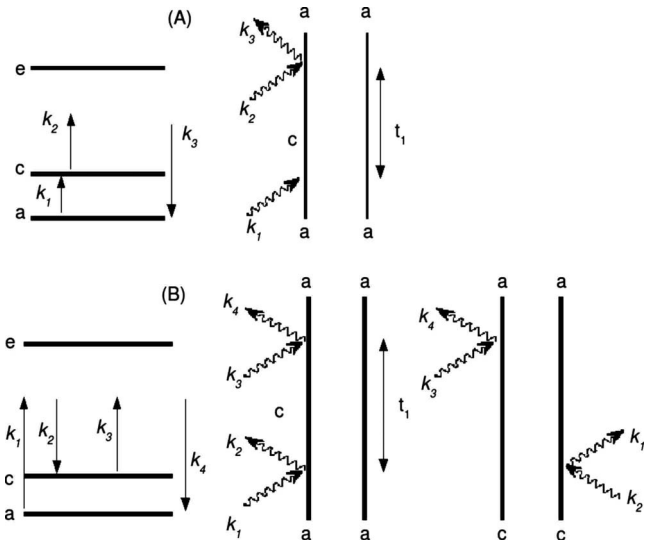

FIG. 2. (a) Level-scheme and Feynman diagram for the IR/Raman sum-frequency-generation $\chi^{(2)}$ process [Eq. (9)]. (b) Level-scheme and Feynman diagrams for the EOR CARS ($\chi^{(3)}$ process) [Eq. (13)].

$$f_{32}(\omega_{ca}) = \frac{1}{2\pi}\int d\omega \varepsilon_2(\omega)\varepsilon_3^*(\omega+\omega_{ca}) \tag{10}$$

is a two-photon spectral density.[15,30]

If the heterodyne field ε_3 bandwidth is narrow (compared to ε_2) and is centered at frequency ω, we have $f_{32}(\omega_{ca})=\varepsilon_3^*(\omega)\varepsilon_2(\omega-\omega_{ca})$. Substituting this in Eq. (9), we obtain the frequency-dispersed heterodyne signal

$$S_{\mathrm{SFG}}(\Omega_1,\omega) = \mathrm{Im}\sum_{a,c} P(a)\frac{\alpha_{ca}V_{ca}\varepsilon_3^*(\omega)\varepsilon_2(\omega-\omega_{ca})\varepsilon_1(\omega_{ca})}{\Omega_1-\omega_{ca}}. \tag{11}$$

This is a 2D spectrum. The envelope of ε_1 selects transitions ω_{ca} within its bandwidth. The dispersed-frequency ω of the signal field enters through the ε_2 and ε_3 pulse envelopes, as in Eq. (A16). Integrating over ω [see Eq. (6)] turns it into a 1D technique [Eq. (9)] which contains phase information.

C. Infrared/Raman/Raman pulse sequence

It is straightforward to include additional IR or EOR pulses in our modular approach and design more elaborate pulse sequences. By adding another optical pair of pulses to the SFG sequence Eq. (9) [Fig. 1(b)] we obtain the $\chi^{(4)}$ process involving one IR and two pairs of EOR pulses. This signal, generated in the direction $\mathbf{k}_5=\mathbf{k}_1+\mathbf{k}_2-\mathbf{k}_3+\mathbf{k}_4$, is given by

$$S^{(4)}(\Omega_2,\Omega_1) = \mathrm{Im}\sum_{a,c,d} P(a)\frac{\alpha_{ad}\alpha_{dc}V_{ca}f_{54}(\omega_{da})f_{32}(\omega_{dc})\varepsilon_1(\omega_{ca})}{(\Omega_1-\omega_{ca})(\Omega_2-\omega_{da})} + \mathrm{Im}\sum_{a,c,d} P(a)\frac{\alpha_{ad}\alpha_{dc}V_{ca}f_{54}(\omega_{dc})f_{32}(\omega_{da})\varepsilon_1(\omega_{ca})}{(\Omega_1-\omega_{ca})(\Omega_2-\omega_{cd})}. \tag{12}$$

As in Eq. (9), if the heterodyne field ε_5 is narrow band (compared to ε_4) and centered at frequency ω we have $f_{54}(\omega_{vv'})=\varepsilon_4(\omega-\omega_{vv'})\,\varepsilon_5^*(\omega)$, turning Eq. (12) into a 3D technique where the signal depends on Ω_1, Ω_2, and ω. Even-order signals ($\chi^{(2)}$, $\chi^{(4)}$, etc.) vanish for isotropic bulk ensembles and are most adequate for probing oriented molecular assemblies or interfaces. $\chi^{(4)}$ is a multidimensional extension of SFG.

D. Raman/Raman pulse sequence; CARS

This $\chi^{(3)}$ process involves one EOR pair followed by a third off-resonant pulse to generate the signal at $\mathbf{k}_4=\mathbf{k}_1-\mathbf{k}_2+\mathbf{k}_3$ [Fig. 2(b)].[18,37] For frequency integrated heterodyne detection we apply Eq. (A9) twice to get

$$S_{\mathrm{CARS}}(\Omega_1) = \mathrm{Im}\sum_{ac}[P(a) - P(c)]\frac{\alpha_{ac}\alpha_{ca}}{\Omega_1-\omega_{ca}}f_{43}(\omega_{ca})f_{21}(\omega_{ca}), \tag{13}$$

with the polarizability

$$\alpha_{ca} = \sum_e \frac{V_{ce}V_{ea}}{\omega_1-\omega_{ec}}, \tag{14}$$

and

$$\alpha_{ac} = \sum_e \frac{V_{ae}V_{ec}}{\omega_4-\omega_{ea}}. \tag{15}$$

The frequency-dispersed detection Eq. (A16) which uses a narrow-band local-oscillator (field ε_4) is recovered by setting $f_{43}(\omega_{ca})=\varepsilon_4^*(\omega)\varepsilon_3(\omega-\omega_{ca})$.

$$S_{\mathrm{CARS}}(\Omega_1,\omega) = \mathrm{Im}\sum_{a,c}[P(a)-P(c)] \times \frac{\alpha_{ac}\alpha_{ca}}{\Omega_1-\omega_{ca}}\varepsilon_4^*(\omega)\varepsilon_3(\omega-\omega_{ca})f_{21}(\omega_{ca}). \tag{16}$$

The ω dependence turns this 1D [Eq. (13)] into a 2D technique [Eq. (16)]. The numerator then contains the Raman ω_{ca} resonances imprinted on the ω axis, as permitted by the ε_4 bandwidth. When ε_3 is broadband, f_{43} becomes flat, independent of ω, and this reduces to the 1D result. CARS resonances can be observed by using a combination of narrow and broadband pulse and spectrally dispersing the signal.[15–19] Note, however, that in Eq. (16) the same resonance ω_{ca} shows up along both Ω_1 and ω frequency axes so that there are no "crosspeaks," and the extra dimensionality does not provide new information in this case. Equation (16) can be alternatively derived starting with the frequency-domain expression for the signal field.

$$S_{\mathrm{CARS}} = \mathrm{Im}\int d\omega_1 d\omega_2 d\omega_3 \chi^{(3)}_{\mathrm{CARS}}(-\omega_s;\omega_3-\omega_2,\omega_1), \quad \varepsilon_1(\omega_1)\varepsilon_2^*(\omega_2)\varepsilon_3(\omega_3)\varepsilon_4^*(\omega)\delta(\omega_1-\omega_2+\omega_3-\omega_s). \tag{17}$$

For our level scheme, (Fig. 1), the third order CARS susceptibility is

$$\chi^{(3)}_{\mathrm{CARS}}(-\omega_s;\omega_3,-\omega_2,\omega_1) \times \sum_{acee'} \frac{P(a)V_{ae'}V_{e'c}V_{ce}V_{ea}}{(\omega_1-\omega_2+\omega_3-\omega_{e'a})(\omega_1-\omega_2-\omega_{ca})(\omega_1-\omega_{ea})} - \frac{P(c)V_{ce'}V_{e'a}V_{ae}V_{ec}}{(\omega_3-\omega_4+\omega_1-\omega_{e'c})(\omega_3-\omega_4-\omega_{ac})(\omega_3-\omega_{ec})}. \tag{18}$$

Equation (16) is obtained by performing the ω_1 and ω_2 integrations and eliminating the ω integral using the δ function.

E. Raman/Raman/Raman pulse sequence: Fifth-order-Raman

This 2D technique (Fig. 3) represents a $\chi^{(5)}$ process involving three pairs of EOR excitation pulses followed by a detection pulse.[8–11] The heterodyne signal generated at $\mathbf{k}_6=\mathbf{k}_1-\mathbf{k}_2+\mathbf{k}_3-\mathbf{k}_4+\mathbf{k}_5$ is calculated by applying Eq. (A9) three times, and is given by

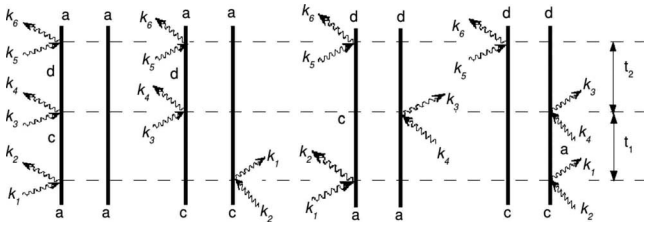

FIG. 3. The four Feynman diagrams contributing to the fifth order Raman $\chi^{(5)}$ process [Eq. (19)].

$$S^{(5)}(\Omega_2,\Omega_1) = \mathrm{Im}\sum_{acd}[P(a)-P(c)]\frac{\alpha_{ad}\alpha_{dc}\alpha_{ca}}{(\Omega_2-\omega_{da})(\Omega_1-\omega_{ca})} \times f_{65}(\omega_{ad})f_{43}(\omega_{dc})f_{21}(\omega_{ca}) + \mathrm{Im}\sum_{acd}[P(a)-P(c)]\frac{\alpha_{ad}\alpha_{dc}\alpha_{ca}}{(\Omega_2-\omega_{cd})(\Omega_1-\omega_{ca})} \times f_{65}(\omega_{dc})f_{43}(\omega_{da})f_{21}(\omega_{ca}). \quad (19)$$

Each transition is now controlled by a corresponding two-photon pulse spectral density. Again, for a narrow band local-oscillator field (ε_6) we set $f_{65}(\omega_{vv'}) = \varepsilon_6^*(\omega)\varepsilon_5(\omega-\omega_{vv'})$ and recover the frequency-dispersed 3D signal with an extra dimension $(\Omega_1,\Omega_2,\omega)$.

In summary, we have used four integrals [Eqs. (A2), (A9), (A16), and (A18)] to dissect the multipoint integrations in Eq. (7) and derive closed expressions for various signals generated by sequences of temporally well-separated pulses. Each resonant IR pulse in Eq. (8) simply selects transitions within its bandwidth. In an EOR process, on the other hand, the Raman transition (ω_{ca}) is resonant, but the intermediate state (ω_{ae}) is not. The process is then described by a two-photon spectral density. We have demonstrated that the dimensionality of the signal may be increased by dispersing the signal or by tuning of a narrow-bandwidth pulse. The same goals may also be achieved by pulse shaping.

ACKNOWLEDGMENTS

The support from the Chemical Sciences, Geosciences and Biosciences Division, Office of Basic Energy Sciences, Office of Science, and U.S. Department of Energy is gratefully acknowledged. I wish to thank Brit Hyland for useful comments.

APPENDIX: USEFUL INTEGRATIONS FOR RESPONSE AND DETECTION

The expressions given below will be used to break up the multiple integrations in Eq. (7), as warranted in various applications.

(i) Resonant interaction with an IR pulse. This involves an integral of the type

$$I_1 = \int_{-\infty}^{t} d\tau V_{ca}(\tau)\varepsilon(\tau). \quad (A1)$$

The upper limit generally extends to the next pulse [see Eq. (7)]. However, for well-separated pulses we can safely extend this limit to $+\infty$ since the pulse envelopes guarantee the required time ordering. This gives[26]

$$I_1 \cong V_{ca}\int_{-\infty}^{\infty}\varepsilon(\tau)\exp(i\omega_{ca}\tau) = V_{ca}\varepsilon(\omega_{ca}). \quad (A2)$$

Equation (A2) implies that only transitions ω_{ca} whose frequency lies within the pulse bandwidth are allowed in this case.

(ii) Off-resonant Raman processes.

Here we have two successive time-ordered interactions, well separated from all others, but not with respect to each other. These require integrals of the form

$$I_{ca}^{21} = \int_{-\infty}^{\tau_3} d\tau_2 \int_{-\infty}^{\tau_2} d\tau_1 \varepsilon_2(\tau_2)\varepsilon_1^*(\tau_1)V_{ce}(\tau_2)V_{ea}(\tau_1). \quad (A3)$$

τ_1 and τ_2 could be any pair of successive time variables in Eq. (7). Since interactions with fields 1 and 2 are not well separated temporally, we can only set τ_3, (but not τ_2) to ∞. By changing variables to $\tau_1=\tau-s$, $\tau_2=\tau+s$, Eq. (A3) is recast in the form

$$I_{ca}^{21} = V_{ce}V_{ea}\int_{-\infty}^{\infty} d\tau \int_{0}^{\infty} ds \varepsilon_2(\tau+s)\varepsilon_1^*(\tau-s), \exp[i\omega_{ca}\tau + i(\omega_{ce}+\omega_{ae})s]. \quad (A4)$$

A Fourier transform of the fields

$$\varepsilon(\tau) = \frac{1}{2\pi}\int d\omega \exp(-i\omega\tau)\varepsilon_2(\omega) \quad (A5)$$

results in

$$I_{ca}^{21} = \frac{1}{2\pi}V_{ce}V_{ea}\int_{-\infty}^{\infty} d\tau \int_{0}^{\infty} ds \int d\omega \times \int d\omega' \varepsilon_2(\omega)\varepsilon_1^*(\omega'), \exp[i(\omega_{ca}+\omega-\omega')\tau + i(\omega_{ce}+\omega_{ae}+\omega+\omega')s]. \quad (A6)$$

The τ integration now gives $2\pi\,\delta(\omega_{ca}+\omega-\omega')$. We can then carry out the s integration to obtain

$$I_{ca}^{21} = \frac{1}{2\pi} V_{ce} V_{ea},$$

$$\int d\omega \int d\omega' \varepsilon_2(\omega) \varepsilon_1^*(\omega') \delta(\omega_{ca} + \omega - \omega') \times \frac{1}{\omega_{ce} + \omega_{ae} + \omega + \omega'}. \tag{A7}$$

The ω' integration gives

$$I_{ca}^{21} = \frac{1}{2\pi} V_{ce} V_{ea} \int d\omega \frac{\varepsilon_2(\omega) \varepsilon_1^*(\omega + \omega_{ca})}{2(\omega - \omega_{ec})}. \tag{A8}$$

Since both pulses are EOR, the denominator is slowly varying and can be taken out of the integration to finally yield

$$I_{ca}^{21} \cong i \alpha_{ca} f_{12}(\omega_{ca}). \tag{A9}$$

Here

$$\alpha_{ca} = \sum_e \frac{V_{ce} V_{ea}}{\omega - \omega_{ec}} \tag{A10}$$

is an effective polarizability and

$$f_{12}(\omega_{ca}) = \frac{1}{2\pi} \int d\omega \varepsilon_2(\omega) \varepsilon_1^*(\omega + \omega_{ca}) \tag{A11}$$

is a two-photon spectral density.[11,30]

Equations (A2) and (A9) are analogous; all we need is replace μ by α, and ε by f. An important difference is that in the IR the pulse envelope $\varepsilon_j(\omega)$ selects positive frequencies and $\varepsilon_j^*(\omega)$ selects negative frequencies. These can be distinguished by the relevant phase matching wave vector $+\mathbf{k_j}, -\mathbf{k_j}$, respectively. In the Raman case, in contrast, the bandwidth of $f_{jg}(\omega)$ spans positive and negative frequencies and both contribute to $\mathbf{k_i} - \mathbf{k_j}$. Within the rotating wave approximation (RWA) the signal then contains additional terms, since phase matching is less selective.

(iii) Off-resonant Raman detection.

If the last interaction is an EOR process, we need the following integral:

$$J_{ac}^j(\omega) = \int_{-\infty}^{\infty} d\tau_2 \exp(i\omega\tau_2) \times \int_{-\infty}^{\tau_2} d\tau_1 V_{ae}(\tau_2) V_{ec}(\tau_1) \varepsilon_j(\tau_1). \tag{A12}$$

Proceeding as before we get

$$J_{ac}^j(\omega) = \frac{1}{2\pi} V_{ae} V_{ec} \int_{-\infty}^{\infty} d\tau_2 \int_{-\infty}^{\tau_2} d\tau_1 \int d\omega_1, \exp[i(\omega_{ae} + \omega)\tau_2 + i(\omega_{ec} + \omega_1)\tau_1] \varepsilon_j(\omega_1). \tag{A13}$$

Setting $s = \tau_2 - \tau_1$ gives

$$J_{ac}^j(\omega) = V_{ae} V_{ec} \int_{-\infty}^{\infty} d\tau_2 \int_0^{\infty} ds \int d\omega_1, \varepsilon_j(\omega_1) \exp[\, i(\omega_{ae} + \omega + \omega_{ec} + \omega_1)\tau_2) - i(\omega_{ec} + \omega_1)s]. \tag{A14}$$

The τ_2 integration gives $2\pi\, \delta(\omega_{ac} + \omega + \omega_1)$. We can then carry out the ω_1 integral and get

$$J_{ac}^j(\omega) = V_{ae} V_{ec} \varepsilon_j(\omega_{ca} - \omega) \times \int_0^{\infty} ds \exp[-i(\omega_{ec} + \omega_{ca} - \omega)s]. \tag{A15}$$

This finally gives

$$J_{ac}^j(\omega) \cong i \alpha_{ac} \varepsilon_j(\omega_{ca} - \omega) \tag{A16}$$

with

$$\alpha_{ac} = \sum_e \frac{V_{ae} V_{ec}}{\omega - \omega_{ea}}. \tag{A17}$$

In heterodyne detection we combine the signal field with a much stronger local-oscillator field $\varepsilon_k(\omega)$ and integrate over frequency. This results in the following quantity:

$$\frac{1}{2\pi} \int J_{ac}^j(\omega) \varepsilon_k(\omega) d\omega = I_{ac}^{jk} f_{jk}(\omega_{ca}). \tag{A18}$$

The imaginary part of Eq. (A18) is detected. Equation (A16) represents a spectrally dispersed signal. Equation (A18) is not dispersed but retains the phase information of the signal. Note that for integrated detection we have

$$\int \varepsilon(t) P^{(n)}(t) dt = \int \varepsilon(\omega) P^{(n)}(\omega) d\omega. \tag{A19}$$

This yields Eq. (6).

[1] A. Laubereau and W. Kaiser, Rev. Mod. Phys. **50**, 607 (1978).
[2] S. M. George, A. L. Harris, M. Berg, and C. B. Harris. J. Chem. Phys. **80**, 83 (1984).
[3] S. Mukamel, *Principles of Nonlinear Optical Spectroscopy* (Oxford University Press, New York, 1995).
[4] K. A. Nelson and E. P. Ippen, Adv. Chem. Phys. **75**, 1 (1989); L. Dhar,

J. A. Rogers, and K. A. Nelson, Chem. Rev. (Washington, D.C.) **94**, 157 (1994).
[5] S. Mukamel, A. Piryatinski, and V. Chernyak, Acc. Chem. Res. **32**, 145 (1999).
[6] J. C. Deak, S. T. Rhea, L. K. Iwaki, and D. D. Dlott, J. Phys. Chem. A **104**, 4866 (2000).
[7] Y. Tanimura and S. Mukamel, J. Chem. Phys. **99**, 9496 (1993).
[8] L. Kaufman, J. Heo, L. D. Ziegler, and G. R. Fleming, Phys. Rev. Lett. **88**, 207402 (2002).
[9] S. Saito and I. Ohmine, J. Chem. Phys. **119**, 9073 (2003).
[10] C. J. Milne, Y. Li, and R. J. D. Miller, in *Time Resolved Spectroscopy in Complex Liquids*, edited by R. Torre (Springer-Verlag, Berlin, 2007), p. 1.
[11] Y. L. Li, L. Huang, R. J. D. Miller, T. Hasegawa, and Y. Tanimura, J. Chem. Phys. **128**, 234507 (2008).
[12] R. F. Loring and S. Mukamel, J. Chem. Phys. **83**, 2116 (1985).
[13] M. Muller, K. Wynne, and J. D. W. Van Voorst, Chem. Phys. **125**, 225 (1988).
[14] L. J. Muller, D. Vandenbout, and M. Berg, J. Chem. Phys. **99**, 810 (1993).
[15] D. Oron, N. Dudovich, D. Yelin, and Y. Silberberg, Phys. Rev. A **65**, 043408 (2002).
[16] D. Pestov, G. O. Ariunbold, X. Wang, R. K. Murawski, V. A. Sautenkov, A. V. Sokolov, and M. O. Scully, Opt. Lett. **32**, 1725 (2007).
[17] D. Pestov, R. K. Murawski, G. O. Ariunbold, X. Wang, M. Zhi, A. Sokolov, V. A. Sautenkov, Y. V. Rostovtsev, A. Dogariu, Y. Huang, and M. O. Scully, Science **316**, 265 (2007).
[18] D. Pestov, X. Wang, G. O. Ariunbold, R. K. Murawski, V. A. Sautenkov, A. Dogariu, A. V. Sokolov, and M. O. Scully, Proc. Natl. Acad. Sci. U.S.A. **105**, 422 (2008).
[19] P. Kukura, D. W. McCamant, and R. A. Mathies, Annu. Rev. Phys. Chem. **58**, 461 (2007).
[20] Z. Chen, Y. R. Shen, and G. A. Somorjai, Annu. Rev. Phys. Chem. **53**, 437 (2002).
[21] K. B. Eisenthal, Chem. Rev. (Washington, D.C.) **96**, 1343 (1996).
[22] G. L. Richmond, Chem. Rev. (Washington, D.C.) **102**, 2693 (2002).
[23] M. Sovago, K. R. Campen, G. W. H. Wurpel, M. Muller, H. J. Bakker, and M. Bonn, Phys. Rev. Lett. **100**, 173901 (2008).
[24] J. Bredenbeck, A. Ghosh, and M. Smits, J. Am. Chem. Soc. **130**, 2152 (2008).
[25] A. Moran, S. Park, and N. F. Scherer, Chem. Phys. **341**, 344 (2007).
[26] I. Schweigert and S. Mukamel, Phys. Rev. A **77**, 033802 (2008).
[27] F. Fournier, E. M. Gardner, D. A. Kedra, P. M. Donaldson, R. Guo, S. J. Butcher, I. R. Gould, K. R. Willison, and D. R. Klug, Proc. Natl. Acad. Sci. U.S.A. **105**, 15352 (2008).
[28] W. Zhao and J. C. Wright, J. Am. Chem. Soc. **121**, 10994 (1999).
[29] C. Dorrer, N. Belabas, J. P. Lickforman, and M. Joffre, J. Opt. Soc. Am. B **17**, 1795 (2000).
[30] T. Brixner, I. V. Stiopkin, and G. R. Fleming, Opt. Lett. **29**, 884 (2004).
[31] W. P. Deboeij, M. S. Pshenichnikov, and D. A. Wiersma, Chem. Phys. Lett. **238**, 1 (1995).
[32] S. Mukamel, Annu. Rev. Phys. Chem. **51**, 691 (2000).
[33] N. Ji, V. Ostroverkhov, C. Y. Chen, and Y. R. Shen, J. Am. Chem. Soc. **129**, 10056 (2007).
[34] A. N. Bordenyuk and A. V. Benderskii, J. Chem. Phys. **122**, 134713 (2005).
[35] I. V. Stiopkin, H. D. Jayathilake, A. N. Bordenyuk, and A. V. Benderskii, J. Am. Chem. Soc. **130**, 2271 (2008).
[36] X. Chen, T. Yang, S. Kataoka, and P. S. Cremer, J. Am. Chem. Soc. **129**, 12272 (2007).
[37] H. Li, D. A. Harris, B. Xu, P. J. Wrzesinski, V. V. Lozovoy, and M. Dantus, Opt. Express **16**, 5499 (2008).